

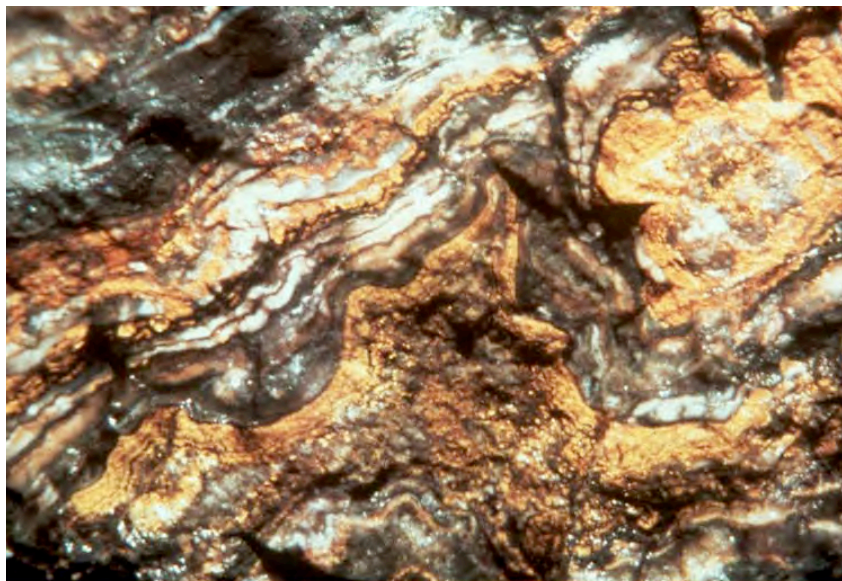
**Geochronology of Volcanic-Hosted Low-Sulfidation Au-Ag Deposits,
Winnemucca-Sleeper Mine area, Northern Great Basin, USA**

**FINAL REPORT
USGS Grant# 05HQGR0153**

“Research supported by the U.S. Geological Survey (USGS), Department of the Interior, under USGS award number 05HQGR0153. The views and conclusions contained in this document are those of the authors and should not be interpreted as necessarily representing the official policies, either expressed or implied of the U.S. Government.”

**James A. Saunders and Willis E. Hames
Department of Geology and Geography
210 Petrie Hall
Auburn University
Auburn, AL 36849**

**Phone: 334-844-4884; FAX: 334-844-4486
EMAIL: saundja@auburn.edu**



High Grade (Bonanza) Ore From the Sleeper Deposit, Nevada

Executive Summary

A number of volcanic-hosted, low-sulfidation Au-Ag deposits were sampled in northern Nevada and southwestern Idaho to collect samples for high-precision ^{40}Ar - ^{39}Ar age dating using the Auburn Noble Isotope Mass Analysis Laboratory (ANIMAL). Ore samples from probable mid-Miocene deposits containing visible precious-metal minerals were collected in 2005 and 2006. The deposits included: 1) three different veins on War Eagle Mountain, Silver City district (Owyhee Mountains, Idaho); 2) a number of deposits in Humboldt County, Nevada, including National and Buckskin National deposits (National district), Sleeper, Jumbo, New Alma, and Sandman in or near the Slumbering Hills, and the Tenmile and Golden Amethyst deposits just northwest of the town of Winnemucca; and 3) two deposits in Elko County: new underground working on bonanza veins at the Midas and Ivanhoe deposits. Adularia (KAlSi_3O_8) is common in some of these deposits and two of the deposits sampled have existing and recent published high-quality Ar-Ar geochronology (Sleeper, Midas). For this study, four other deposits were chosen for detailed geochronology because of the coarse-grained nature of adularia and its intimate association in the ores with precious-metal minerals: Jumbo, New Alma, Sandman, and Tenmile deposits. Laser $^{40}\text{Ar}/^{39}\text{Ar}$ incremental heating plateau ages for single crystals of adularia from these mines as obtained thus far range from 16.51 ± 0.04 Ma to 15.91 ± 0.03 Ma (at the 1-sigma uncertainty level), a time period that is consistent with a possible genetic link to the Yellowstone hotspot. This research is the basis of a M.Sc. thesis at Auburn University, and three peer-reviewed papers are anticipated that use some data supported by this research grant (one has been submitted, two are in preparation).

Introduction

A genetic association between mid-Miocene volcanic-hosted epithermal gold-silver deposits and the mantle plume of the Yellowstone hotspot was proposed by Saunders et al. (1996), John et al. (1999) and John (2001). This study was proposed to provide geochronology of epithermal Au-Ag deposits in the northern Nevada for which age dates for ore formation are completely lacking, were done by older techniques (e.g., K-Ar), or where definitive textural data were lacking for unambiguously linking timing of gold mineralization with the mineral(s) dated. Further, we hypothesized that existing age dating, which predominantly had been conducted on larger deposits, might have biased the interpretation of timing and duration of precious metal mineralization perhaps associated with the Yellowstone hotspot. Thus, we visited a number of prospects, historic producers, and relatively newly discovered and recently producing deposits that we could obtain permission to sample. One of the prospects (Sandman) was the site of 100 new exploration drill holes in 2006 and may become an economic resource.

Volcanic-Hosted Epithermal Precious-Metal Deposits

Many epithermal deposits were study in detail in the 1800's and early 1900's by such eminent USGS scientists as Lindgren, Ransome, and Spurr. Indeed the term "epithermal" deposit was coined by Waldemar Lindgren, who also discovered the mineral adularia which he observed to be a common gangue mineral in these ores (Lindgren, 1898). Lindgren (1900) also recognized the relatively rare mineral naumannite (Ag_2Se) that is presently the second-most abundant ore mineral in these northern Great basin deposits after electrum (Halsor et al., 1988; Vikre, 1985; Saunders, 1994; Saunders et al., 1996; Bussey, 1996; Goldstrand and Shmidt, 2000; John, 2001; Leavitt et al., 2004). Early researchers noticed the close association (in time and

space) with volcanic rocks and thus they assumed that the epithermal ores were genetically associated with such volcanics. The advent of light-stable isotope investigations of epithermal ores from 1950's through 1980's led many to propose that the nearby intrusions only acted as heat sources for the shallow hydrothermal systems, and that the geothermal fluids leached metals from surrounding country rocks. However, by the early 1990's, it became increasingly apparent (again!) that the magmas were indeed the source of the metals as Lindgren and colleagues had originally proposed as far back as a century earlier. For example Saunders (1988, 1991) proposed that epithermal gold telluride deposits in Colorado were formed by magmatic fluids from alkalic intrusions sourced from the mantle. Hedenquist and Lowenstern (1994); Heinrich et al. (1999) and Sillitoe and Hedenquist (2003) presented substantial new data and developed new models for formation of epithermal deposits from magmatic fluids. For example, Hedenquist Lowenstern (1994) laid out the geologic and geochemical framework demonstrating how subvolcanic intrusions are genetically related to deeper porphyry and shallower epithermal ores (Fig. 1).

In the new model of Hedenquist and Lowenstern (1994) loss of volatiles from magmas could form large but low-grade "porphyry" stockwork deposits (or skarns) of $\text{Cu} \pm \text{Au} \pm \text{Mo}$ within or adjacent to the subvolcanic intrusions. If structural and/or hydrologic conditions favored, metal-rich magmatic fluids could move upward and, outward to form either the rock-buffered,

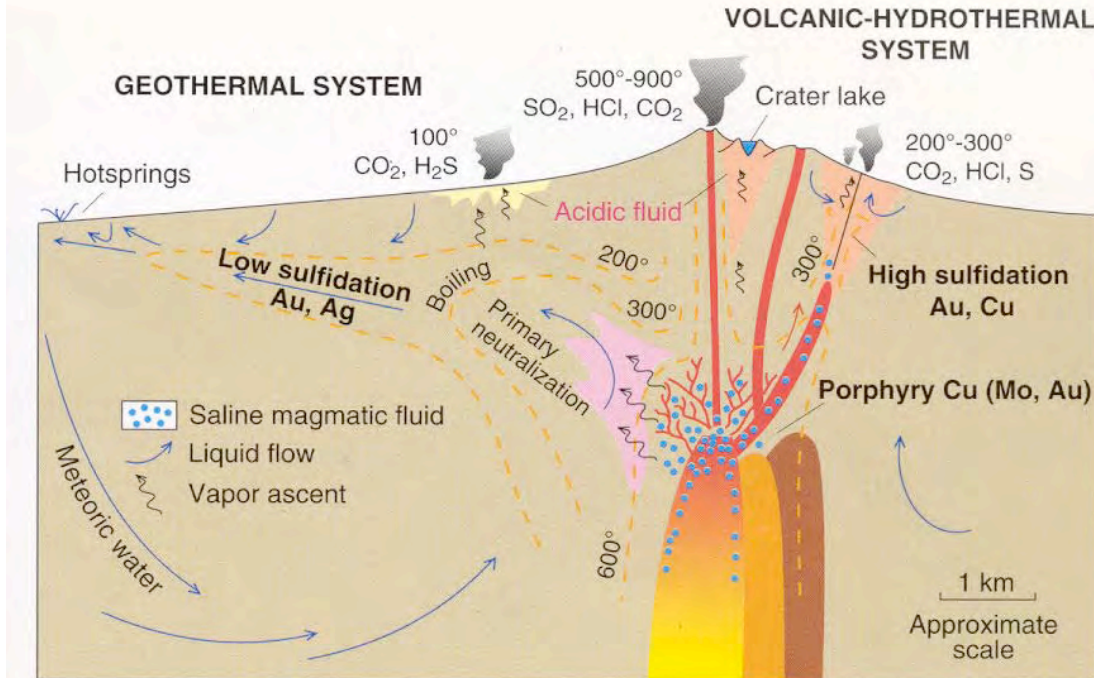


Figure 1. Diagrammatic model of relationship of low-sulfidation and high-sulfidation to co-genetic subvolcanic intrusions and associated porphyry-style ores, modified from Hedenquist and Lowenstern (1994).

neutral-pH, reduced (e.g., H₂S as the dominant S species) low sulfidation (LS) epithermal deposits, or the high-sulfidation (HS) deposits formed from acidic, oxidized fluids (SO₂ or SO₄ dominant S species) and associated extensive advanced-argillic alteration. The model also explained many features of present-day geothermal systems (e.g., their predominant water compositions and distribution, and their chemical evolution by mixing and boiling). One potential problem with the concept that magmatic fluids could move upward from the source magmas was that these fluids were known to be very highly saline (e.g., the ones documented in high-temperature porphyry Cu-Mo deposits) and thus very dense. But Hedenquist and Lowenstern (1994) also showed that it is possible that an immiscible low-density (vapor-rich) fluid could separate from the saline magmatic fluid, and this could explain the occurrence of metal-rich super-critical fumaroles such as those noted at White island, New Zealand

(Giggenbach, 1992). Not long after the Hedenquist-Lowenstern model was published, striking supporting evidence was found in a fluid inclusion study of the world-class Grasberg-Ertsberg porphyry Cu-Au deposit at Papua, New Guinea. Heinrich et al. (1999), using new laser-ablation ICP-MS fluid inclusion microanalysis technology found evidence that a low-density, vapor-rich fluid had separated from dense, saline magmatic fluids there (in the porphyry environment) and that this fluid contained high concentrations of sulfur, copper, and gold (>10 ppm Au!). This discovery, and subsequent papers demonstrating the potential significance of how such low-density, S-Cu-Au-rich fluids could move out of the deeper “porphyry” environment to form shallower epithermal systems, provide the framework for the current models for the origin of epithermal deposits and their connection to deeper, magmatic hydrothermal processes.

Volcanic-hosted LS deposits in northern Nevada are typically mid-Miocene in age and have been proposed to be related to the Northern Nevada Rift (John et al., 1999; John, 2001; Ponce and Glen, 2002; Grauch et al., 2003; Leavitt et al., 2004) and/or the Yellowstone hotspot (Saunders et al., 1996; John et al., 1999; John, 2001). John (2001) proposed that epithermal deposits in NV can be subdivided into extension-related deposits associated with bi-modal volcanics in central NV, and subduction-related deposits associated with andesites in western Nevada. Further, John proposed that the extension-related deposits are associated with magmas of low water content and reducing in nature, whereas the subduction-related deposits are related to water-rich, oxidized magmas. There are also some important HS deposits in the subduction-related ores, whereas they are absent in the rift-related deposits (John, 2001).

Of the mid-Miocene LS epithermal deposits in the NGB (Fig. 2), the Sleeper deposit (Sunders 1990, Conrad et al., 1993, Saunders, 1994, Saunders and Schoenly, 1995, Nash et al., 1995), National-Buckskin National deposits (Vikre, 1985, 1987) and Midas (Gol dstrand and

Schmidt, 2000, Leavitt et al., 2004) are the best documented. In addition, DeLamar (Halsor et al., 1988), Hog Ranch (Bussey, 1996), Mule Canyon (John, et al., 2003)

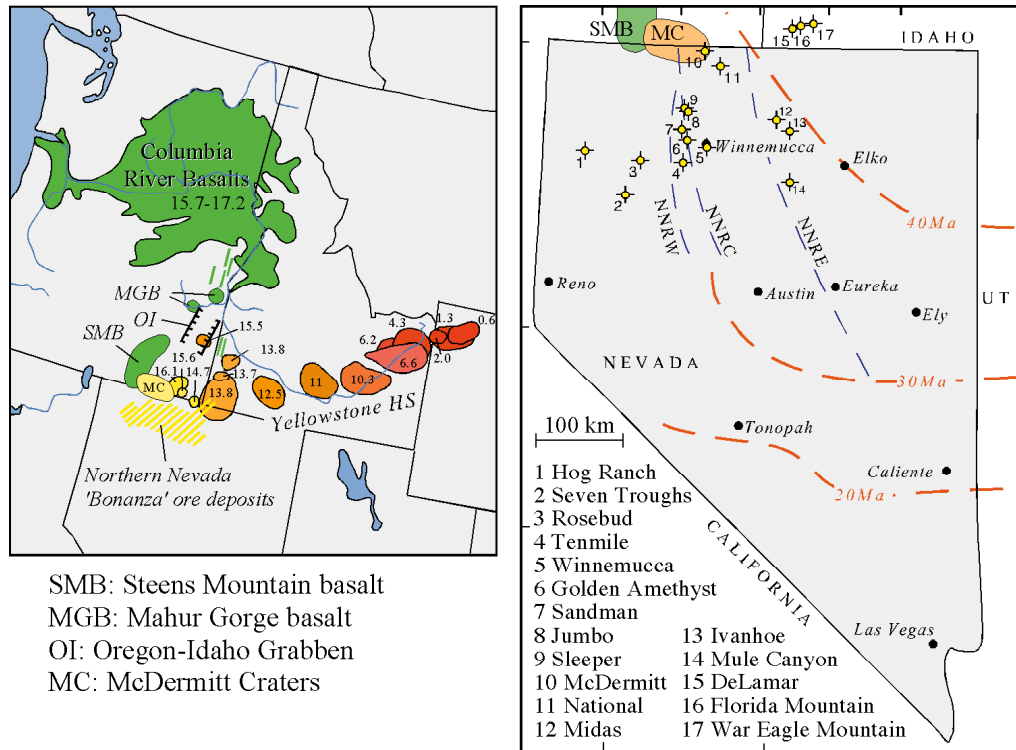


Figure 2a: Ages of calderas in the Yellowstone hotspot track and basalts (green) and the Columbia River flood basalt province. Fig. 2b: Locations for many of the 17-14 Ma LS epithermal deposits in NGB (modified from Saunders et al. 1996), through-going structures as defined by geophysical data and the regional trend (dashed contours) of Cenozoic-subduction magmatism (John et al., 1999; Ponce and Glenn, 2002; Grauch et al., 2003; Leavitt et al., 2004). New Alma deposit (not shown) is approximately 1.5 km south of Jumbo (no. 8).

and Ivanhoe (Wallace, 2003) each have one or more papers that describe them in detail. The close association of the LS in the northern Great Basin with the bimodal volcanics have led some (Noble et al., 1988; Connors et al., 1993) to propose that the deposits are genetically related (e.g., Au-Ag coming from magmatic fluids mixing with meteoric waters) to the coeval magmatism. Recent detailed investigations in the Santa Rosa range (east of the Sleeper deposit and continuing northward to the National district, and almost to the McDermitt caldera; Fig. 2) by Brueseke and

Hart (2004) reinforces the connection of mid-Miocene volcanism with the Yellowstone hotspot, but demonstrates that the “bimodal” volcanism is not as bimodal as previously thought, at least in their study area (numerous intermediate compositions were found).

Previous Geochronology

(This section on previous geochronology is reproduced from the original proposal for USGS Grant#05HQGR0153 as originally submitted in 2005 by Saunders and Hames.)

A number of K/Ar and $^{40}\text{Ar}/^{39}\text{Ar}$ age determinations have been published for the Miocene bonanza-type Au-Ag mineralized deposits of northern Nevada (Table 1). The data available suggest a maximum interval of ca. 13-17 Ma for mineralization in these deposits, with much of the primary mineralization appearing to occur in the interval 14-16.5 Ma. It is also generally accepted that at about 16.5-17.5 Ma the impingement of a small mantle plume at the base of the lithosphere in the Nevada-Oregon-Idaho tri-state region led to the origin of both the Yellowstone hotspot and the Columbia River flood basalt province (Hooper, 1997). Although the majority of Columbia River flood basalt magmatism occurred further north, the earliest, picritic basalts of the province have been identified at Steens Mountain, and the original distribution of the Steens basalt overlaps the McDermitt craters (Fig. 1). Thus, the bonanza deposits of northern Nevada

Table 1. Compilation of Ages of NGB Volcanic-Hosted Low Sulfidation Au-Ag (Hg) Ores*

Deposit	Deposit Number (Fig. 1)	Age (K-Ar or Ar-Ar) Ma
Hog Ranch	1	15.2-14.8
Seven Troughs	2	14.1
Tenmile	4	16.7
Jumbo	8	17.3
Sleeper	9	16.1-15.5
National/Buckskin National	11	15.6
McDermitt (Hg)	10	15.6
Midas	12	15.1-15.2
Ivanhoe	13	15.2
Mule Canyon	14	15.6
DeLamar	15	15.7

**Data compiled from Vikre (1985), Halsor (1988), Conrad et al., (1993), Bussey (1996), Saunders et al. (1996), John (2001), John et al. (2003), Leavitt et al. (2004), and Wallace (2003).*

may be broadly coincident in time and space with the earliest magmatism of the Yellowstone hotspot and Columbia River flood basalt province.

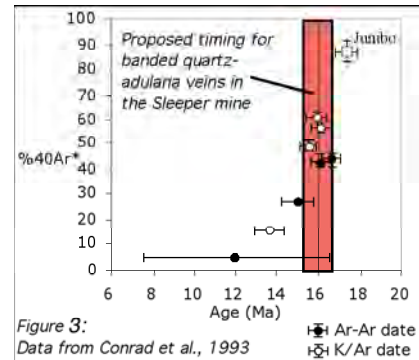
Studies such as that of Conrad et al. (1993) and John (2001) have done a great deal to provide solid benchmarks for the general timing and age relationships for a few of the bonanza ores of northern Nevada. However, additional work that utilizes more precise methods is needed to compare the timing of ore genesis among the deposits and to place this timing in a broader geodynamic context. Bulk-sample total-fusion (K/Ar and $^{40}\text{Ar}/^{39}\text{Ar}$) techniques as used in most of the published studies (see Table 1) are inherently limited because of their inability to resolve the potential contributions from various sources of extraneous argon (inherited 'excess' ^{40}Ar , or other non-atmospheric argon). The data of Conrad et al.

(1993) for high-grade ore samples is reproduced in Figure 3 to illustrate the limitations in data presently available.

Conrad et al. (1993) present data for five samples of high-grade ore: three bulk samples of adularia+quartz from banded ore of the Sleeper mine, one adularia+quartz sample from

brecciated secondary ore in the Sleeper mine, and a sample of coarse adularia from the nearby Jumbo mine. Separate splits of the samples from the Sleeper mine were prepared by K/Ar and $^{40}\text{Ar}/^{39}\text{Ar}$ total fusion.

In the K/Ar and $^{40}\text{Ar}/^{39}\text{Ar}$ total-fusion methods as applied by Conrad et al. (1993), a single age determination is essentially a model age, corrected for extraneous, or 'excess' ^{40}Ar on the basis of an assumed $(^{40}\text{Ar}/^{39}\text{Ar})_{\text{ex}} = 295.5$ (the ratio in the present atmosphere). In Figure 2 ages are plotted against the percentage of radiogenic ^{40}Ar for the analysis; analyses with lower radiogenic yields are subject to larger corrections for extraneous argon. The brecciated ore



samples gave the youngest ages, the oldest ages were for the banded ore, and Conrad et al. (1993) interpreted that the high-grade mineralization at the Sleeper mine began at ca. 16.2 Ma and was of about 1 m.y. duration, with some hydrothermal activity and remobilization of ores continuing to ca. 14 Ma. We believe this interpretation is logical and consistent with the data. However, note that there is a tendency for the analyses with lower radiogenic yield to define younger ages. Such a tendency for younger ages could arise through two different processes: 1) secondary weathering or hydrothermal alteration among the samples could have leached radiogenic ^{40}Ar and/or enriched potassium; and, 2) the extraneous argon (perhaps cited in fluid inclusions) may have had $^{40}\text{Ar}/^{36}\text{Ar}$ ratios lower than that of modern atmosphere (ratios as low as 284 have been observed in certain volcanic and hydrothermal systems, e.g., McDougall and Harrison, 1988), and thus the typical atmospheric model ‘overcorrects’ the data. Note that the sample of coarse adularia from the Jumbo mine has a radiogenic yield of ca. 87% and an age of ca. 17.3 Ma. Conrad et al. (1993) interpreted this to indicate that mineralization at the Jumbo mine occurred earlier than at the Sleeper mine. However, the data also permits the interpretation that if samples from the Sleeper mine had been characterized by higher radiogenic yields, the age of primary mineralization at Sleeper could in fact be closer to 17 Ma than 15-16 Ma, and the ores of the two mines would be of the same age and more consistent with their proximity.

The precise absolute ages, and relative differences on the order of 1-2 m.y., are important to resolve because they can place the deposits in the geodynamic framework of the region (Cenozoic extension, calc-alkaline subduction magmatism, mantle plume impingement and hot-spot volcanism, etc.) as well as to enhance exploration. The $^{40}\text{Ar}/^{39}\text{Ar}$ incremental heating technique has dramatically increased success in geochronologic studies of ore deposits (as discussed by Snee, 2003). The most significant enhancements from the incremental heating

method are the ability to detect disturbed or complex argon distributions (particularly important where there is a potential for effects of weathering, alteration, or fine-grained mixtures in bulk samples) and that the method allows measurement and more robust correction for extraneous argon. Such methods have been applied recently to Miocene deposits in southern Nevada that are related to subduction magmatism (Berger et al., 1999; Vikre et al., 2003). The laser $^{40}\text{Ar}/^{39}\text{Ar}$ techniques of $^{40}\text{Ar}/^{39}\text{Ar}$ dating offer the further advantage to analyze very small amounts of sample material (typically two to three orders of magnitude less material than with the more standard ‘resistance-furnace’ incremental heating techniques) and the corrections for system backgrounds and extraneous argon can be applied more accurately. Laser $^{40}\text{Ar}/^{39}\text{Ar}$ dating provides a significant advantage for dating economic deposits when potassium-bearing minerals (adularia, illite, etc.) are rare or very finely grained (as discussed by Hall et al., 1997). For our study, we used laser $^{40}\text{Ar}/^{39}\text{Ar}$ facilities in the Auburn Noble Isotope Mass Analysis Laboratory (ANIMAL, as described in the appendix for Facility Descriptions), that are optimized for incremental heating and replicate fusion analysis of micro-samples.

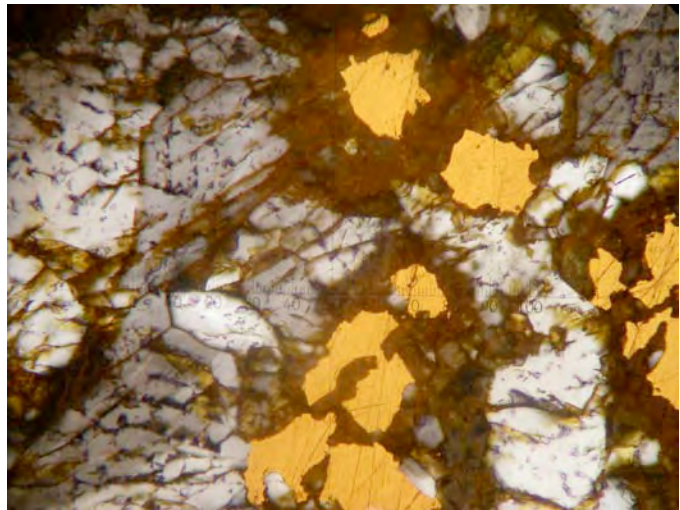
Procedure

Fieldwork was conducted during two different trips to Nevada in 2005 and 2006. Ore samples from probable mid-Miocene deposits containing visible precious-metal minerals were collected and described in the field, and locations were determined by GPS. The deposits sampled included: 1) a number of deposits in Humboldt County, Nevada, including National and Buckskin National deposits (National District), Sleeper, Jumbo, New Alma, and Sandman in or near the Slumbering Hills, and the Tenmile and Golden Amethyst deposits (just northwest of the town of Winnemucca); 2) three different veins on War Eagle Mountain, in the Silver City district

(Owhyhee Mountains, Silver City, Idaho); and 3) two deposits in Elko County: new underground working on bonanza veins at the Midas and Ivanhoe deposits.

Samples were returned to Auburn University for petrographic analysis of vein mineralization, and samples containing coarse-grained adularia intergrown with ore minerals (e.g., Fig. 4) were selected for detailed geochronology. Adularia was separated by hand picking single crystals, typically in the range of 100-200 μm in diameter. The single crystals selected for laser analysis were generally subhedral, or cleavage fragments, free from visible inclusions of other phases, and were generally free from alteration. All samples were washed in dilute HF

Figure 4. Photomicrograph taken in reflected and transmitted light of intergrown electrum (gold) and adularia (gray) from the Jumbo Deposit, Slumbering Hills, Nevada. Textures indicate simultaneous deposition of the minerals. Note this sample is slightly weathered, and contains iron oxides, though the adularia is very fresh. Field of view is 1 mm.



prior to analysis, which was useful in removing oxides (limonite coatings) from some weathered samples. Neutron irradiation for the production of ^{39}Ar followed standard procedures as described by Dalrymple et al. (1981), using the central core facility of the McMaster Nuclear Reactor in Hamilton, Ontario. Crystals were packed in aluminum disks with the monitor FC-2 (age = 28.02 Ma, Renne et al., 1998) and reagent grade K_2SO_4 and CaF_2 as flux monitors. We experimented with three approaches to laser extraction and analysis of data: 1) laser fusion for a number of single crystals (typically 10), and data analysis on standard isotope correlation diagrams; 2) two-step extraction for a number of single crystals (an initial, low power step

followed by fusion) with data analysis on isotope correlation diagrams; and, 3) laser incremental heating of single crystals to generate a release spectrum (by regulating laser output power, with 8 or more steps per analysis), and data reduction through both the model-age spectrum and isotope correlation diagram approaches. We used the Isoplot program (Ludwig, 2003) for all final data reduction and assessment of statistical ages.

Results

Table 2 summarizes ages obtained thus far in the project, through two-step release of argon from single crystals and analysis of data on an isotope correlation diagram (listed as ‘2-step’), and through incremental heating and generation of an age spectrum for single crystals (listed as ‘spectrum’). For the data obtained through the incremental heating release spectrum approach (method #3 from above), the samples yielded plateau ages essentially identical to the ages obtained by regression. In general, the samples are characterized by high radiogenic yields, with the combined percentage of radiogenic argon ranging from ~ 85-99%. The initial, or trapped, components of extraneous argon in each sample were of atmospheric composition, within uncertainty.

Ages for Adularia presently obtained through USGS Grant #05HQGR0153					
Sample	Mine	Type of Age	% ⁴⁰ Ar*	Age	
HCN-3RE	Jumbo	plateau	98.6	16.442	± 0.020
HCN-3RE	Jumbo	isochron	98.1	16.630	± 0.390
HCN-3OX	Jumbo	plateau	98.0	16.091	± 0.028
HCN-3OX	Jumbo	isochron	98.4	16.150	± 0.410
HCN-1	Adularia Hill	isochron	85.5	16.230	± 0.060
HCN-1	Adularia Hill	isochron	87.7	16.190	± 0.120
HCN-2	New Alma	isochron	98.5	16.100	± 0.700
HCN-2	New Alma	plateau	98.9	15.910	± 0.027
HCN-4	Tenmile	plateau	90.1	16.513	± 0.046

Our logic behind the two-step analyses was that the first step would preferentially release any extraneous ^{40}Ar in the crystal, and the second step would be predominated by radiogenic argon produced in the crystal. While this proved a valid approach, the resulting errors obtained through regression of such data had precisions ranging from 0.06—0.7 Ma (at one sigma, the analyses labeled ‘2-step’) whereas the ages determined by the incremental heating approach (labeled ‘spectrum’) ages had precisions within about 0.05 Ma. We are presently obtaining incremental heating data on additional crystals from each sample, in order to assess the precision and inherent variability among adularia crystals from single samples and veins.

Note that different results were obtained for two crystals from the Jumbo mine. Sample HCN-3RE, a ‘reduced’ sample without evidence of weathering or oxidation, yielded a plateau age of 16.44 ± 0.02 Ma, whereas a more ‘oxidized’ sample from the same outcrop (HNC-3OX) yielded a statistically younger plateau age of 16.09 ± 0.03 Ma (with similar, though less precise, results for the 2-step analyses and the isochron approach). This might result can be interpreted to indicate loss of radiogenic ^{40}Ar from crystals in sample HCN-3OX during late-stage, oxidizing conditions (through weathering or high temperature hydrothermal alteration), or that there is geologic age variability of ca. 0.35 Ma among adularia crystals as sampled from the Jumbo mine. We prefer the former explanation, although we re-collected samples from the Jumbo mine in the summer of 2006 and are presently completing analyses to test these two explanations.

Age spectra for the four incremental heating spectrum analyses of table 2 are presented in figure 5. Each of these spectra represents data obtained from a single adularia crystal. Three of the samples (Figure 4A-C, from Jumbo and New Alma) have plateau defined by all increments (100% of the released ^{39}Ar), whereas the crystal analyzed from Tenmile contains a small proportion of non-atmospheric ‘excess’ argon. (The default plateau requirements of Isoplot were

used — plateau increments constitute more than 60% of released $^{39}\text{Ar}_K$, no discernable slope among plateau increments, contiguous increments yield the same ages within their standard deviation — comparable to the rigor of definitions in many other studies.)

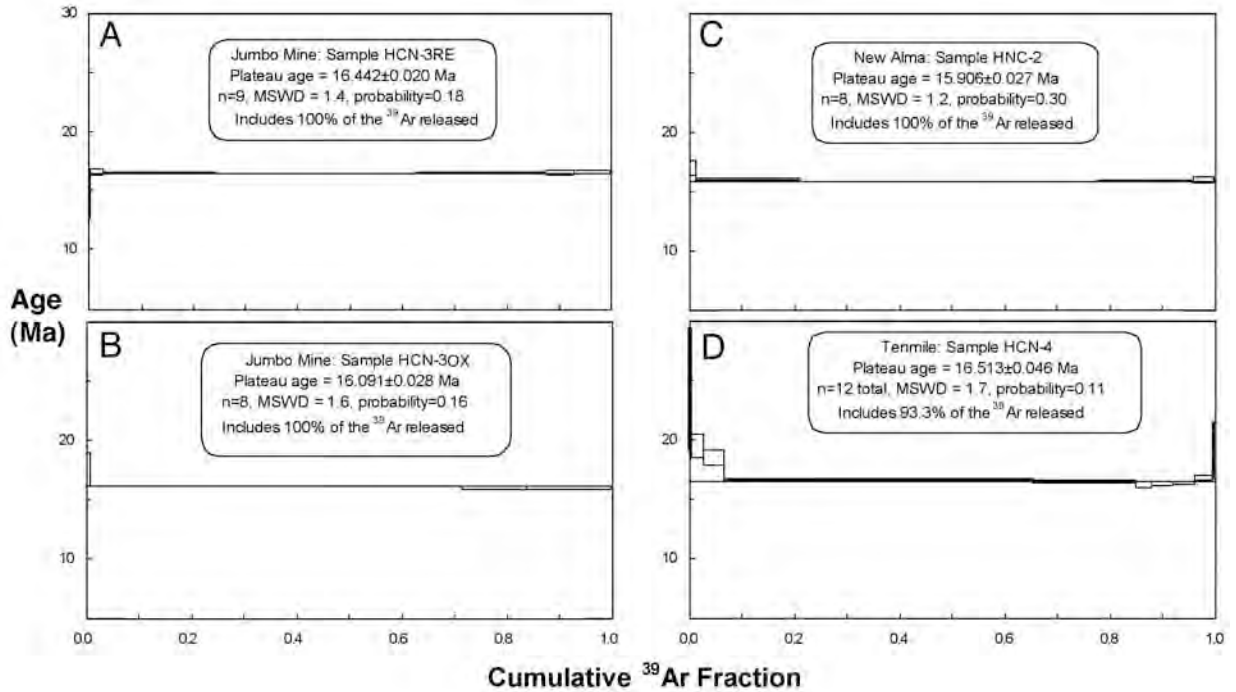
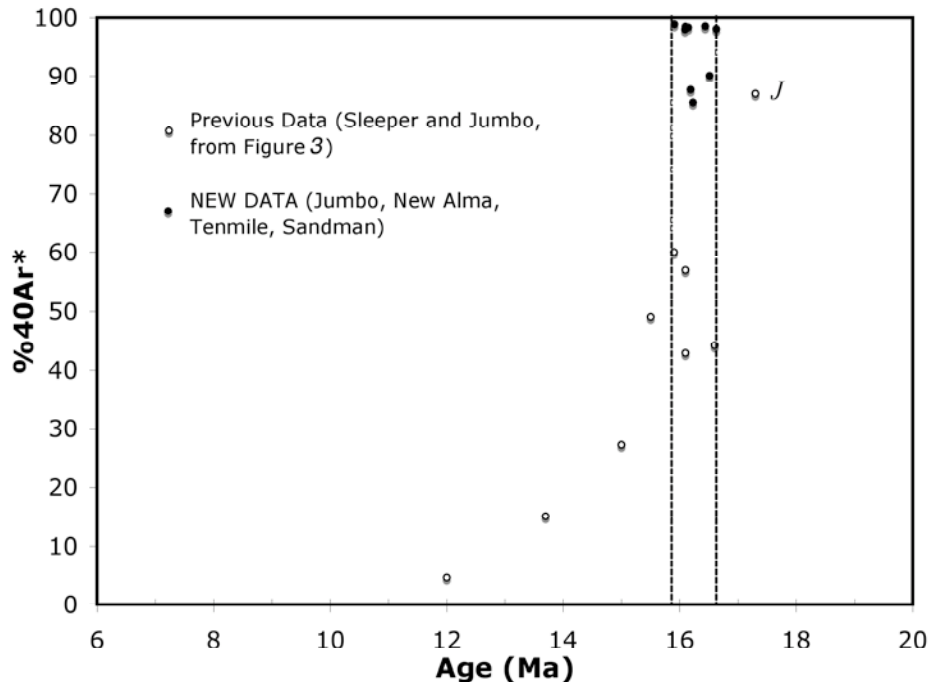


Figure 5: $^{40}\text{Ar}/^{39}\text{Ar}$ incremental heating release spectra for single crystals of adularia from. 4A, Jumbo mine, sample HCN-3RE, with a plateau age of 16.44 ± 0.2 Ma (all ages quoted at the $1\text{-}\sigma$ level); 4B, Jumbo Mine, sample HCN-3OX, with a plateau age of 16.09 ± 0.03 Ma; 4C, New Alma mine, sample HCN-2, with a plateau age of 15.91 ± 0.3 Ma; and, 4D Tenmile mine, sample HCN-4, with a plateau age of 16.51 ± 0.05 Ma.

The results of our investigations as obtained thus far are summarized in Figure 6, which presents the data reported in Conrad et al. (1993) for Sleeper and Jumbo (c.f. Figure 3 of this report) along with data obtained thus far in this study for Jumbo, New Alma, Tenmile, and Sandman (i.e., all of the ages reported in Table 2). The laser analytical methods used in the present study yielded ages characterized by radiogenic yields that are higher than typical of previous work. Note also, in comparison with Figure 3, that the ages we obtain for adularia of four different bonanza ores is very comparable to that inferred for Sleeper and Jumbo by

Figure 6: Ages vs. radiogenic yields for all ages of Table 2, delimited by the dashed vertical lines, compared with previous results from Sleeper and Jumbo ('J') reported in Conrad et al. (1993).



Conrad et al. (1993). Thus, our results suggest all of these ores formed in the approximate interval of 16.5 to 15.9 Ma. These results add considerably to the inference that the bonanza ores of northwest Nevada are coincident in time and space with the initiation of the Yellowstone hotspot and early magmatism of the Columbia River flood basalt province. Previous results for Sleeper that are significantly younger than ~15.9 Ma seem associated with loss of radiogenic argon and incorporation of atmospheric extraneous argon. Similarly, the ~ 17 Ma result reported earlier for a sample from Jumbo ('J' in figure 6) now appears somewhat suspect, as all of the data we have obtained for duplicate samples from Jumbo indicate an age between 16.5 and 16.1 Ma. Furthermore, an age of 17 Ma seems, at this point, to be a rather extraordinary result that would be ~ 0.5 Ma older than the oldest known magmatism of the Yellowstone hotspot (Steens Mountain basalt, ca. 16.5 Ma). Thus, we suggest the earlier result for Jumbo is anomalously old due to an unresolved component of extraneous ^{40}Ar , and note this interpretation should be verified by additional testing.

Conclusions and Implications

High-precision $^{40}\text{Ar}/^{39}\text{Ar}$ incremental heating analyses of adularia intergrown with electrum in four LS epithermal Au-Ag deposits in northern Nevada yield ages in the range of 16.5 to 15.9 Ma for the precious-metal forming events. Results support a close genetic link to magmatism associated with the development of the Yellowstone hotspot in northern Nevada during the mid-Miocene. If this conclusion is correct, then there is the possibility that similar LS Au-Ag deposits may have formed at other localities eastward (perhaps younger, and presently at deeper crustal levels) along the mid-Miocene to present Yellowstone hotspot track.

References Cited

- Bussey, S.D., 1996, Gold mineralization and associated rhyolitic volcanism at the Hog Ranch District, northwest Nevada: *Proceedings of the International Symposium on the Geology and Ore Deposits of the America Cordillera*: (Reno, NV) p. 181-210.
- Brueseke, M.E., and Hart, W.K., 2004, The physical and petrologic evolution of a multi-vent volcanic field associated with Yellowstone-Newberry volcanism: *Eos, Transactions of AGU*, v. 87(47), p. V53A-605.
- Connors, K.A., Noble, D.C., Bussey, S.D. and Weiss, S.I., 1993, Initial gold contents of silicic volcanic rocks: Bearing on the behaviour of gold in magmatic systems, *Geology*, vol.21, p.937-940.
- Conrad, J.E., McKee, E.H., Rytuba, J.J., Nash, J.T., and Utterback, W.C., 1993, Geochronology of the Sleeper deposit, Humboldt, County, Nevada: Epithermal gold-silver mineralization following silicic flow-dome complex: *Economic Geology*, v. 88, p. 317-327.
- Dalrymple, G.B., Alexander, E.C., Lanphere, M.A., and Kraker, G.P., 1981, Irradiation of samples for $^{40}\text{Ar}/^{39}\text{Ar}$ dating using the Geological Survey TRIGA Reactor: USGS Professional Paper 1176, 55 p.
- Giggenbach, W.F., 1992, Magma degassing and mineral deposition in hydrothermal systems at convergent plate boundaries: *Economic Geology*, v. 87, p. 1927-1944.
- Goldstrand, P.M., and Schmidt, K.W., 2000, Geological Society of Geology, mineralization, and ore controls at the Ken Snyder gold-silver mine, Elko County, NV Nevada, *Geology and*

- Ore Deposits, 2000: The great Basin and Beyond Symposium, May 15-18, 200, Reno-Sparks, NV, Proceedings, p.265-287.
- Grauch, V.J.S., Rodriquez, B.D., and Wooden, J.L., 2003, Geophysical and isotopic constraints on crustal structures related to mineral trends in north-central Nevada, and implications for tectonic history: *Economic Geology*, v. 98, p. 287-316.
- Halsor, S.P., Bornhorst, T.J., Beebe, Matt, Richardson, Kim, and Strowd, William, 1988, Geology of the DeLamar silver mine, Idaho-A volcanic dome complex and associated hydrothermal system: *Economic Geology*, v. 83, p. 1159-1169
- Hedenquist, J.W., and Lowenstern, J.B., 1994, The role of magmas in the formation of hydrothermal ore deposits: *Nature*, v. 370, p. 519-527.
- Heinrich, C.A., Gunther, D., Audetat, A., Ulrich, T., and Frischknecht, R. 1999, Metal fractionation between magmatic brine and vapor, determined by microanalysis of fluid inclusions: *Geology*, v. 27, p. 755-758.
- John, D.A., Garside, L.J., and Wallace, A.R., 1999, Magmatic and tectonic setting of Late Cenozoic epithermal gold-silver deposits in northern Nevada, with an emphasis on the Pah Pah and Virginia Ranges and the Northern Nevada Rift: *Geological Society of Nevada Special Publication 29*, p. 64-158.
- John, D.A., 2001, Miocene and early Pliocene epithermal gold silver deposits in the in the northern Great Basin, western USA: Characteristics, distribution, and relationship to magmatism: *Economic Geology*, v. 96, p. 1827-1853.
- John, D.A., Hofstra, A.H., Fleck, R.J., Brummer, J.E., Saderholm, E.C., 2003, Geologic setting and genesis of the Mule Canyon Low-Sulfidation epithermal gold-silver deposit, north-central Nevada: *Economic Geology*, v. 98, p. 425-464.
- Leavitt, E.D., Spell, T.L., Goldstrand, P.M., and Arehart, G.G., 2004, Geochronology of the Midas low-sulfidation gold-silver deposit, Elko County Nevada: *Economic Geology*, v.99, p. 1665-1686.
- Lindgren, W., 1898, Hydrothermal potassium feldspar in gold ores from De Lamar, Idaho: *American Journal of Science: (Fourth Series)* no. 30, p.418-420.
- Lindgren, W., 1900, The gold and silver veins of the Silver City, De Lamar, and other mining districts in Idaho: US Geological Survey 20th Annual Report, Part 3, p. 65-256.
- Ludwig, K.R., 2003, User's manual for Isoplot, v. 3.0, a geochronological toolkit for Microsoft Excel: Berkeley Geochronological Center, Special Publication no. 4.
- Nash, J.T., Utterback, W.C., and Trudel, W.S., 1995, Geology and geochemistry of

- Tertiary volcanic host rocks, Sleeper Gold-Silver deposit, Humboldt County, Nevada:
U.S. Geological Survey Bulletin 2090.
- Noble, D.C., McCormack, J.K., McKee, E.H., Silberman, M.L., and Wallace, A.B.,
1988, Time of mineralization in the evolution of the McDermitt caldera complex,
Nevada-Oregon, and relation to middle-Miocene mineralization in the Great Basin to
coeval regional basaltic activity: *Economic Geology*, v. 83., p. 859-863.
- Ponce, D.A., and Glen, J.M.G., 2002, Relationship of epithermal gold deposits to large-scale
fractures in northern Nevada: *Economic Geology*, v. 97, p. 3-9.
- Renne, P.R., Swisher, C.C., Deino, A.L., Karner, D.B., Owens, T.L., and DePaolo, D.J., 1998,
Intercalibration of standards, absolute ages, and uncertainties in $^{40}\text{Ar}/^{39}\text{Ar}$ dating:
Chemical Geology, v. 145, p. 117-152.
- Saunders, J.A., 1990, Colloidal transport of gold and silica in epithermal precious
metal systems: Evidence from the Sleeper deposit, Humboldt County, Nevada: *Geology*,
v. 18, p. 757-760.
- Saunders, J.A., 1994, Silica and gold textures at the Sleeper deposit, Humboldt County, Nevada:
Evidence for colloids and implications for ore-forming processes: *Economic Geology*, v.
89, p. 628-638.
- Saunders, J.A., and Schoenly, P.A., 1995, Boiling, colloid nucleation and aggregation, and the
genesis of bonanza gold mineralization at the Sleeper Deposit, Nevada: *Mineralium
Deposita*, v. 30, p. 199-211.
- Saunders, J.A., Schoenly, P.A., and Cook, R.B., 1996, Electrum disequilibrium
crystallization textures in volcanic-hosted bonanza epithermal gold deposits: *Proceedings
of the International Symposium on the Geology and Ore Deposits of the America
Cordillera*: (Reno, NV) p. 173-179.
- Sillitoe, R.H., and Hedenquist, J.W., 2003, Linkages between volcanotectonic settings,
ore-fluid compositions, and epithermal precious metal deposits: *Society of Economic
Geologists Special Publication no. 10*, 315-343.
- Vikre, P.G., 1985, Precious metal vein system in the National district, Humboldt County,
Nevada: *Economic Geology*, v. 80, p. 360-393.
- Vikre, P.G., 1987, Paleohydrology of Buckskin Mountain, National district,
Humboldt County, Nevada: *Economic Geology*, v. 882, p. 934-950.
- Wallace, A.R., 2003, Geology of the Ivanhoe Hg-Au district, Northern Nevada: Influence
of Miocene volcanism, lakes, active faulting on epithermal mineralization: *Economic
Geology*, v. 98, p. 409-424.

Appendix: Analytical Facility Description

The Auburn Noble Isotope Mass Analysis Laboratory (ANIMAL) was utilized for age determinations in this study:

- a. This facility is equipped with an ultra-high vacuum, 90-degree sector, 10 cm radius spectrometer optimized for $^{40}\text{Ar}/^{39}\text{Ar}$ research (single-crystal and multigrain sample incremental heating). The spectrometer employs second-order focusing (Cross, 1951), and is fitted with a high sensitivity electron-impact source and a single ETP electron multiplier (with signal amplification through a standard pre-amplifier). Analyses of this study were made using a filament current of 2.250 A, and potentials for the source and multiplier of 2000 V and 1250 V, respectively. The total volume of the spectrometer is 400 cc. Resolution in the instrument (with fixed slits for the source and detector) is constrained to ~ 150 , and the high sensitivity and low blank of the instrument permits measurement of 10^{-14} mole samples to within 0.2% precision. Analyses comprised 10 cycles of measurement over the range of masses and half-masses from $m/e=40$ to $m/e=35.5$, and baseline corrected values were extrapolated to the time of inlet, or averaged, depending upon signal evolution.
- b. The extraction line for this system utilizes a combination of Varian ‘mini’ and Nupro pneumatic valves, and Varian turbomolecular and ion pumps. Analysis of samples and blanks is fully automated and can be controlled via computer. Pumping of residual and sample reactive gases is accomplished through use of SAES AP-10 non-evaporable getters. Pressures in the spectrometer and extraction line, as measured with an ionization gauge, are routinely below $\sim 5 \times 10^{-9}$ torr. A pipette delivers standard aliquots of air for use in measuring sensitivity and mass fractionation. Mass discrimination was typically 1.0026 ± 0.0014 per amu (95% confidence level) in November of 2006.
- c. The extraction line is fitted with a 50W Synrad CO_2 IR laser for heating and fusing silicate minerals and glasses. The sample chamber uses a Cu planchet, KBr cover slips, and low-blank UHV ZnS window (manufactured at Auburn University and based on the design of Cox et al., 2003). In the present configuration, this laser system is suitable for incremental heating and fusion analysis of single crystals and multigrain samples. The laser beam delivery system utilizes movable optical mounts and a fixed sample chamber to further minimize volume and improve conductance of the extraction line. (The time required to inlet, or equilibrate, a ‘half-split’ of a sample is less than 7 s, and the inlet time for a full sample is ca. 20 s.) Typical blanks for the entire system (4 minute gettering time) in November of 2006 are as follows (in moles): ^{40}Ar , 5.7×10^{-17} ; ^{39}Ar , 1.3×10^{-17} ; ^{38}Ar , 2.8×10^{-18} ; ^{37}Ar , 2.0×10^{-18} ; ^{36}Ar , 1.2×10^{-18} .
- d. Computer control of the laser, laser optics, extraction line, mass spectrometer, and data recording is enabled with National Instruments hardware and the Labview programming environment. Initial data reduction is accomplished through an in-house Excel spreadsheet, with final reduction using Isoplot (Ludwig, 2003).

Additional References for the Appendix:

Cross, W.G., 1951, Two-directional focusing of charged particles with a sector-shaped, uniform magnetic field: *Reviews of Scientific Instruments*, v. 22, p. 717-722.

Cox, S.G., Griffin, P.F., Adams, C.S., DeMille, D., and Riis, E., 2003, Reusable ultrahigh vacuum viewport bakeable to 240 C: *Review of Scientific Instruments*, v. 74, no. 6, p. 3185-3187.

Ludwig, K.R., 2003, User's manual for Isoplot, v. 3.0, a geochronological toolkit for Microsoft Excel: Berkeley Geochronological Center, Special Publication no. 4.